POLARIMETRY OF SOLAR PORES

P. SÜTTERLIN, E.H. SCHRÖTER AND K. MUGLACH
Kiepenheuer Institut für Sonnenphysik, Freiburg, Germany

Abstract. We address the magnetic field structure of solar pores. The data were obtained at the Gregory Coudè telescope at Izaña using the AT1 CCD camera system to observe pores with three spectral lines: one magnetically sensitive line, recording all 4 Stokes profiles, and two $g = 0$ lines where only the intensity profiles were measured. The data reduction included the standard procedure (removing dark current and flatfielding) as well as destretching of the polarimetric spectra and removing the non–magnetic straylight by means of a 2–d deconvolution of the observed intensity variation using a Lucy–Richardson restoration algorithm. In the following analysis we first determined the temperature- and pressure stratification of the pore using the $g = 0$ lines and then applied an inversion of the Stokes profiles to get the parameters of the magnetic field. Across the pore we find a strong variation of the resulting field strength as well as of the inclination and the azimuth, consistent with the assumption of a canopy forming in the higher atmosphere.

Key words: Solar magnetic fields – Pores – Polarimetry

1. Introduction

We present an investigation of the internal properties of solar pores using polarimetric spectra. The usual definition of a pore is that it is a sunspot lacking a penumbra but recent high resolution speckle observations (Keller, 1992) as well as the magnetic field variation across the object (Muglach *et al.*, 1994) indicate that this is a rather arbitrary definition. Its brightness should be less than about 80% of the surrounding atmosphere (Brants and Steenbeck, 1985; Muller, 1992). Many contributions have used photometric information only (Bumba, 1967; Beckers and Schröter, 1968; Brants and Zwaan, 1982; Bonet *et al.*, 1994), most of them are hampered by the limited size of the pores and thus the influence of seeing except Bonet *et al.* who use the moon limb for seeing correction.

When interested in their internal properties the use of polarized light has the advantage that it originates in the magnetic part of the observed resolution element and is not mixed with non–magnetic straylight. Information derived from polarimetric measurements can be found in Sütterlin (1991), Thim (1993), Muglach *et al.* (1994) and Sütterlin *et al.* (1994).

We analyse intensity spectra taken in two magnetically insensitive lines in addition to spectra of the complete Stokes vector in a g=2.5 line. An inversion technique is used to determine the thermodynamic and magnetic structure of a pore.

Solar Physics **164**: 311–320, 1996.

2. Instrumental Setup and Observations

The spectra were taken on May 30^{th}, 1993, at the 45-cm Gregory-Coudé-Telescope of the Observatorio del Teide at Izaña, Tenerife. This telescope is well suited for polarimetric observations due to the low instrumental polarization which only depends on the observed declination δ (and is even zero for $\delta = 0$). The focal length of 25 m yields a spatial scale of $8.25''$/mm in the plane of the spectrograph entrance slit. As detector we used the AT1 CCD camera system with a chip of 1024×1024 pixels, each having a size of $19\mu^2$. The linear dispersion of the GCT spectrograph is 1.79Å/cm at 630.2 nm, resulting in a scale of 3.41mÅ $\times$ $0.157''$ on the chip.

The observed object was a pore in the near surroundings of the complex B-group NOAA 7515 and located at $\cos\theta = 0.87$. Under very good seeing conditions, the best spectra show structures down to approximately $0.6''$. Due to this as well as to increase the signal to noise ratio we averaged four spatial rows (giving an image resolution of $0.63''$).

The spectra of the magnetically insensitive lines Fe I 512.3 nm and Fe I 709.0 nm were recorded simultaneously using the so–called spectrum cutter. The Stokes I, Q, U and V spectra of Fe I 630.2 nm (g=2.5) had to be recorded consecutively due to instrumental constraints. For the polarimetric observations we used a device (Soltau, 1993) consisting of two birefringent calcites orientated at $\pm 45°$ relative to the entrance slit of the spectrograph, thereby also setting the local reference frame for the azimuth measurement. Together with a quarter-wave retarder at 0° this device splits the beam into two parts, each of which carrying the information of $\frac{1}{2}(I - V)$ and $\frac{1}{2}(I + V)$, respectively. By projecting the two beams onto the same CCD camera it is possible to simultaneously observe the two polarization states (e.g. $I \pm V$). Stokes Q and U are measured by rotating the quarter-wave plate by 45° (U) and adding a half-wave retarder at 22.5° (Q).

3. Data Reduction

The data reduction consisted of a number of steps, including the standard procedure of subtracting the dark current and flatfielding the image.

The correction for instrumental scattered light introduced by the polarization optics and the spectrum cutter (Thim, 1993) was done by measuring the equivalent widths of solar spectral lines and comparing them to those in a quiet sun FTS atlas compiled by Neckel. Atmospheric scattered light has also to be taken into account. We used the continuum intensity fluctuations along the slit to produce a pseudo-two dimensional intensity image by rotating them around the pore center. This image was then de-convoluted with a seeing function using an iterative Lucy-Richardson restoration algorithm.

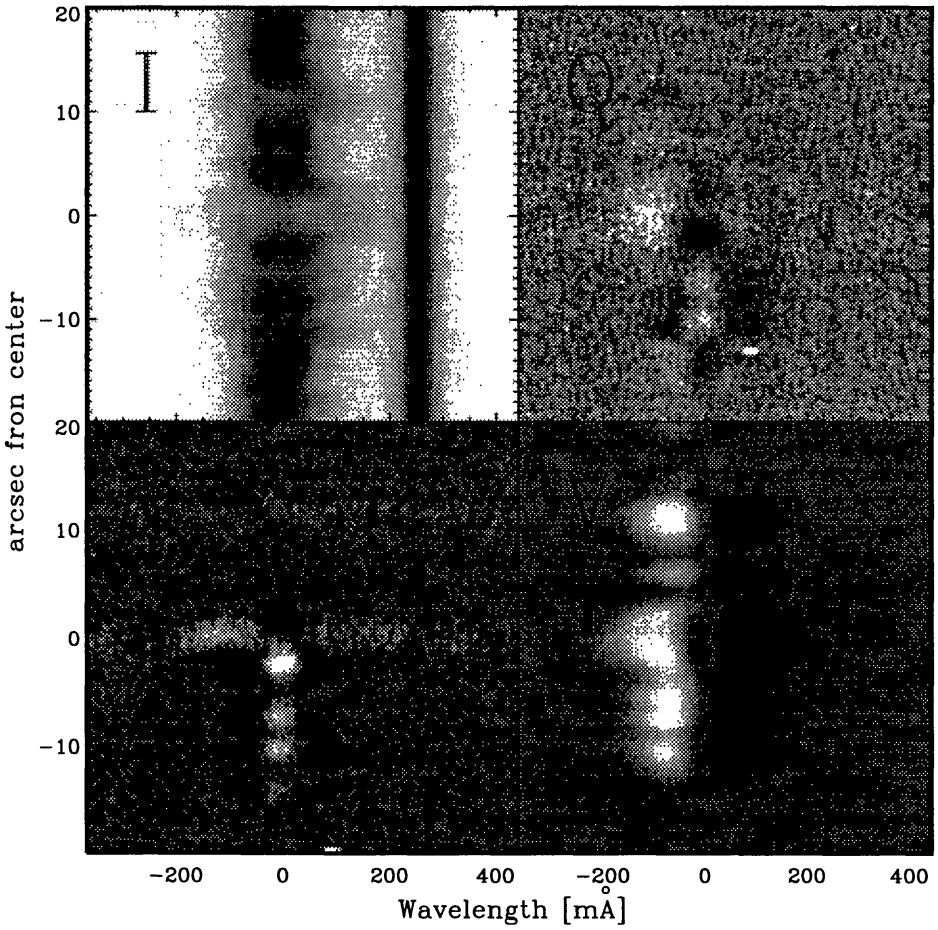

Fig. 1. Reduced and normalized Stokes I, Q, U and V spectra of Fe I 6302.5.

As point spread function we chose an analytical one (Rossbach and Schröter, 1970) which consists of two Gaussians taking into account the influence of image motion and background scattered light. One of them, representing image motion, has a half-width of 0.6″ which was derived from the size of the smallest visible structure in the spectrum.

This algorithm can strictly only be applied if the *complete* information of the observed object is included in the image, which is obviously not the case for the (spatially) one–dimensional spectrum (see Keller and Johannesson, 1995, for a method to circumvent this by means of a rapid scanning across the observed structure). However, there are two points to justify this procedure: First, the surroundings of the pore is granulation, which has a self-similar structure and the pore itself has also an axisymmetric appearance. Therefore the error introduced by taking the same spatial structure in all directions is likely to be small. And second, assuming of a point spread function in itself is quite a constraint. Our resulting continuum intensity at the center of the pore is 28% of the continuum intensity averaged along the slit, which

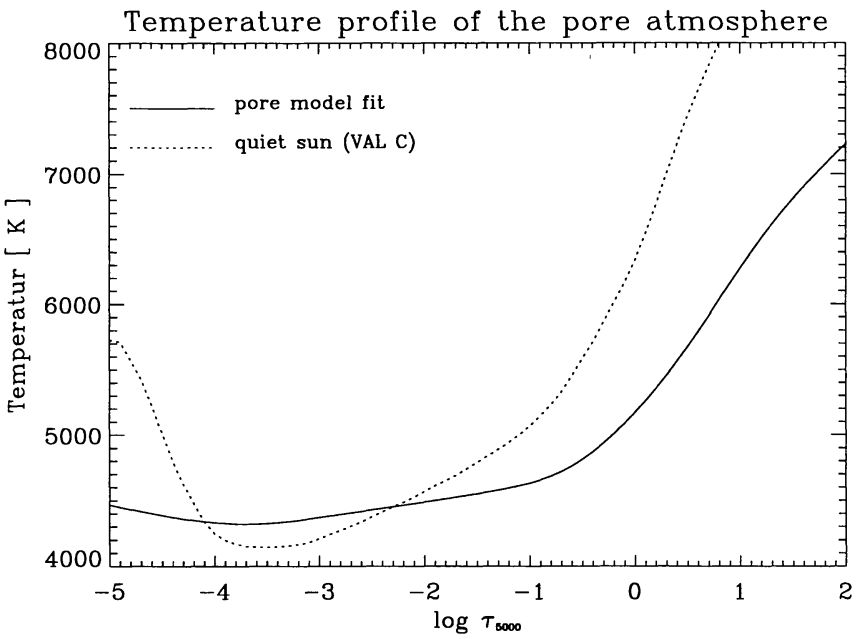

Fig. 2. Temperature as a function of optical depth τ (at $\lambda = 5000$ Å) of the model atmosphere of the pore which we derived from a fit to the two $g = 0$ lines. The solid line represents the pore atmosphere, the dotted one is a model of the quiet sun.

is in good agreement with similar investigations (Sütterlin (1991) gives 31%, Thim (1993) gives 28% and Bonet *et al.* (1994) give a value of 30%).

Then each spectrum was normalized to the local continuum and the best one of each series (determined by the largest continuum rms value and the lowest continuum intensity) was selected for further evaluation.

One additional reduction step was necessary for the polarimetric data: The two polarization states of the image show some spatial degradation caused by the different light paths in the calcites. Therefore the spatial scale had to be adjusted to allow the subtraction of the two parts without introducing artefacts. For this purpose the granular continuum intensity variations were used as tracers for a 1-D local correlation tracking routine.

The reduced Stokes I, Q, U and V spectra of the pore can be seen in Figure 1 as a gray–scale plot.

4. Analysis and Results

Our least square fitting routine applies a Levenberg-Marquardt algorithm to find the minimum in parameter space. To describe the atmosphere we choose a set of 8 parameters: four of them determine its thermodynamic structure (minimum temperature, temperature range, a parameter for the temperature gradient and the gas pressure at the deepest point), the other four the magnetic field (the field strength at $\tau = 1$, the field gradient, linear

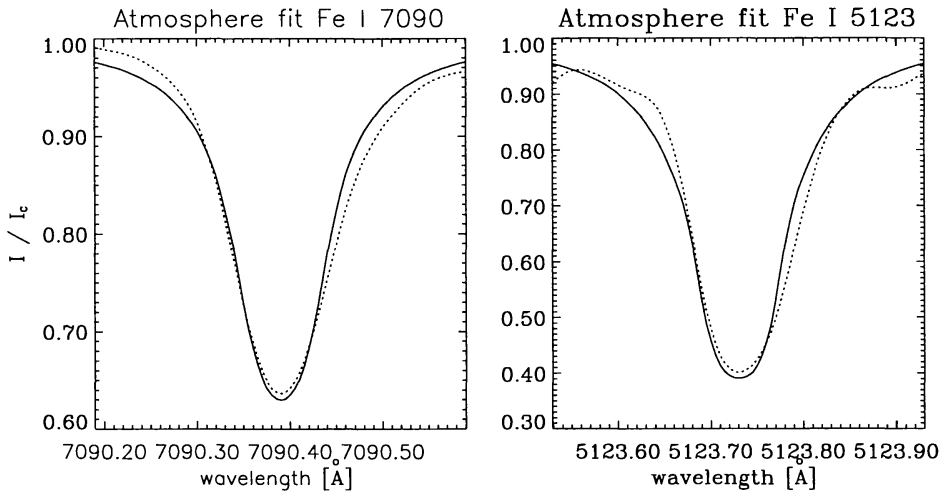

Fig. 3. Fits of the two $g = 0$ lines using the model atmosphere shown above in Figure 2. The dotted line is the measured profile, the solid one represents the best fit.

in $\log \tau$, the inclination and azimuth angle of the field, which are constant with depth in the atmosphere). For a given set of parameters the atmosphere is computed and the radiative transfer equation of the Stokes vector is solved using a code kindly provided by U. Grossmann–Doerth.

The applied inversion of the reduced spectra consists of three steps: First we determine the temperature- and pressure stratification of the pore by fitting the two non-splitting lines. Figure 2 shows the resulting model atmosphere together with a model of the quiet sun (VAL C, Vernazza *et al.*, 1976) and Figure 3 gives the resulting fit of the lines.

In the next step we applied this thermodynamic model to determine the parameters of the magnetic field from the polarization spectra of Fe I 630.2 nm. After test calculations we decided not to try a simultaneous fit of all 4 Stokes parameters. They were not recorded simultaneously and therefore do not show the same orientation of the field vector. Furthermore the accuracy of the azimuth measurement (derived from the linear polarization states) is much less than that of the inclination: The signal to noise ratio of Q and U is worse due to the small signal. In addition the effects of smearing and averaging over a range of magnetic field vectors (introduced both by the finite width of the spectrograph slit and image motion during the exposure) is larger for the azimuth than for the inclination.

It turned out that the fit of the gradient of the magnetic field is not possible when using only one spectral line. Although the gradient tends to broaden the wings of I and V and therefore should be easily detectable, the data are too noisy to give a reliable fit. Therefore we used a fixed increment of 400 Gauss per decade in the logarithmic optical depth scale as field gradient. For our atmosphere, this corresponds to approximately 3.5 Gauss/km.

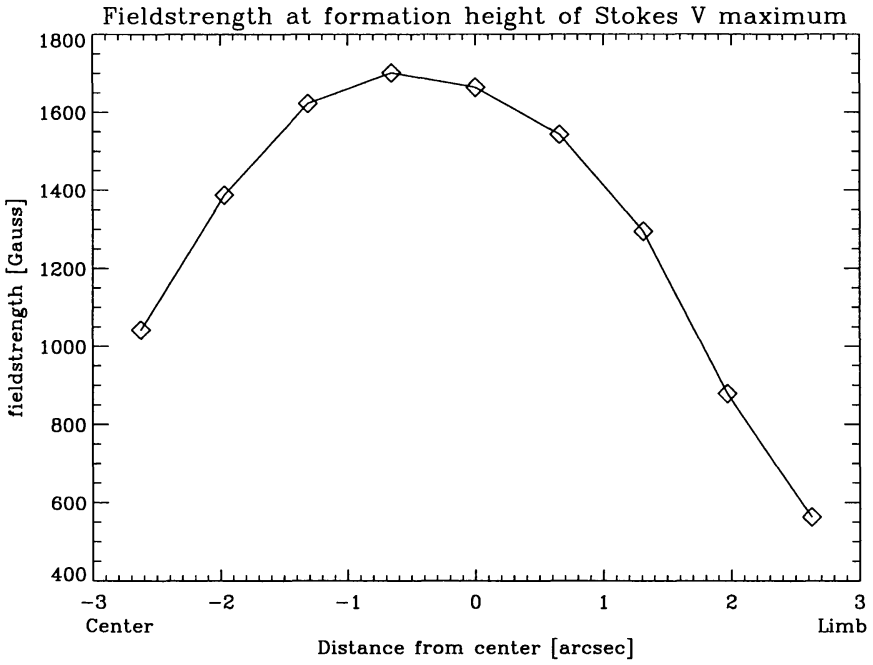

Fig. 4. Field strength B (in Gauss) across the pore. The values were determined from a fit of Stokes I and V of the Fe I 6302.5 Å line. They refer to the height of formation of the Stokes V maximum, which lies around $\log\tau = -2$. The direction of disk center and limb are indicated at the bottom of the plot. A gradient of the field of 3.5 G/km was also included in the model. The size of the pore seen in Stokes V is larger than the size of the visible pore (defined by the points where 90 % of the photospheric intensity is reached) which extends $\pm 2''$ from the central position.

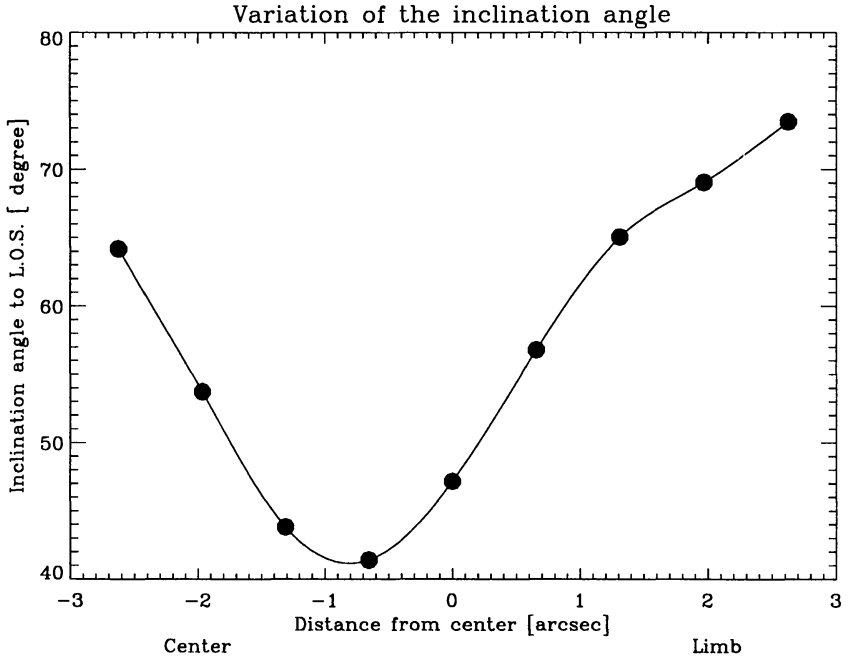

Fig. 5. Inclination angle of the field (with respect to the line of sight) across the pore also determined from a fit to Stokes I and V.

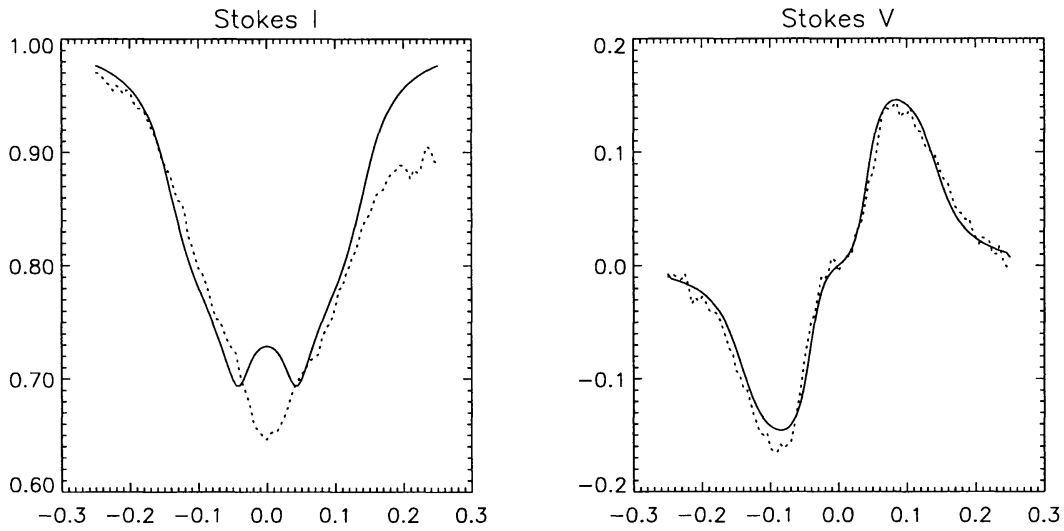

Fig. 6. This figure shows a representative example of the fits to Stokes I and V (the dotted line is the measured profile, the solid one is the fit). The temperature stratification of Figure 2 was used. The field strength and inclination angle of the field were varied to give the best fit.

Fitting Stokes I and V together gives strength and inclination of the field: Figure 4 shows the results for the variation of the field strength across the pore, extrapolated to the height of formation of the 630.2 nm line (at about $\log\tau = -2$ for our atmosphere). The field strength at $\tau = 1$ is about 800 Gauss larger. Figure 5 shows the inversion results for the inclination of the field. The values are not corrected for the position of the pore on the disk, 30°. The fact that $\gamma = 0$ is reached nowhere in the pore is a hint that we did not cut through the center of the pore. An example of the line profiles is shown in Figure 6.

The determination of the azimuth angle of the field also suffers from the fact that the Q and U spectra could not be recorded simultaneously and therefore show different orientations. We decided to drop the Stokes Q measurement and to use only the U spectrum for the fit. In general it is not possible to measure the field azimuth using only one of the linear polarization signals. However, as we fixed all other parameters in earlier stages, there was only one parameter to fit. Adopting a smooth variation of the azimuth across the pore, we used for each spatial point the result of the preceeding fit as the initial value, starting the whole process at the point with maximum U signal. The results given in Figure 7 show a large scatter, the solid line represents a weighted linear regression. If only those points are used where a clear signal had been detected (marked by black dots) one can see the expected smooth variation of the azimuth of nearly 180°. Finally in Figure 8 one can find the complete set of Stokes U profiles and their fits. At

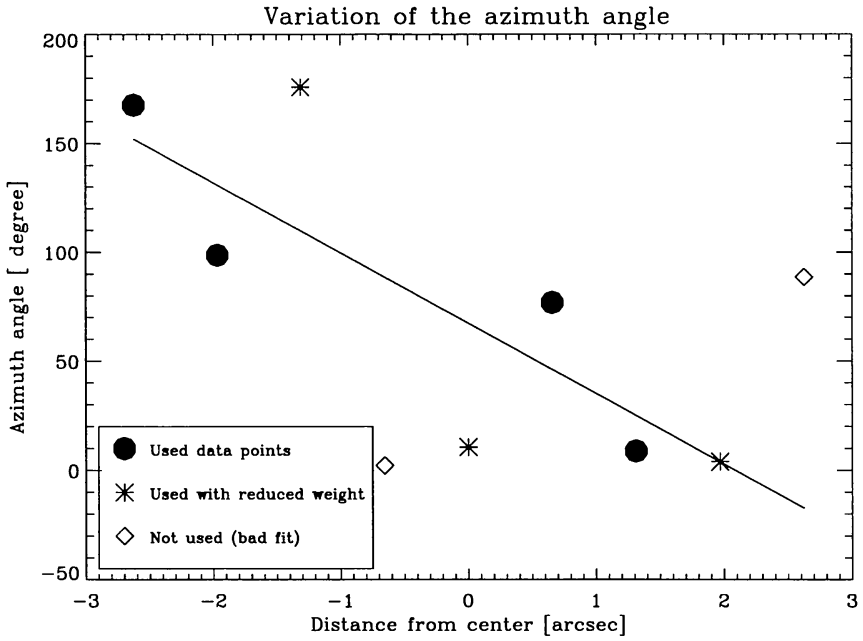

Fig. 7. The azimuth angle ϕ of the magnetic field (in degrees) across the pore is shown which is derived from a fit of Stokes U profiles. The straight line is a weighted linear regression through the points, the weight was selected according to the quality of the fit (see Figure 8).

two positions the U signal almost vanishes, indicating an azimuth of 0 or 90°. Due to the lack of a simultaneous measurement of Stokes Q the code can not distinguish between these two cases.

5. Conclusions and Outlook

This investigation shows that high spatial and spectral resolution polarimetry of small elements is possible and leads to good and consistent results. Additional efforts are required for the determination of the atmospheric straylight, which we plan to do by introducing a filling factor which is then also a parameter to be fitted, and using absolute intensity profiles. There is also a clear need to observe magnetically sensitive lines with different heights of formation simultaneously. In this case the gradient of the field strength can be determined with $< 20\%$ error, as tests with synthetic data have shown.

Acknowledgements

We wish to thank U. Grossmann-Doerth, who kindly supplied his radiative transfer code for the computation of the full Stokes vector, and S.K. Solanki

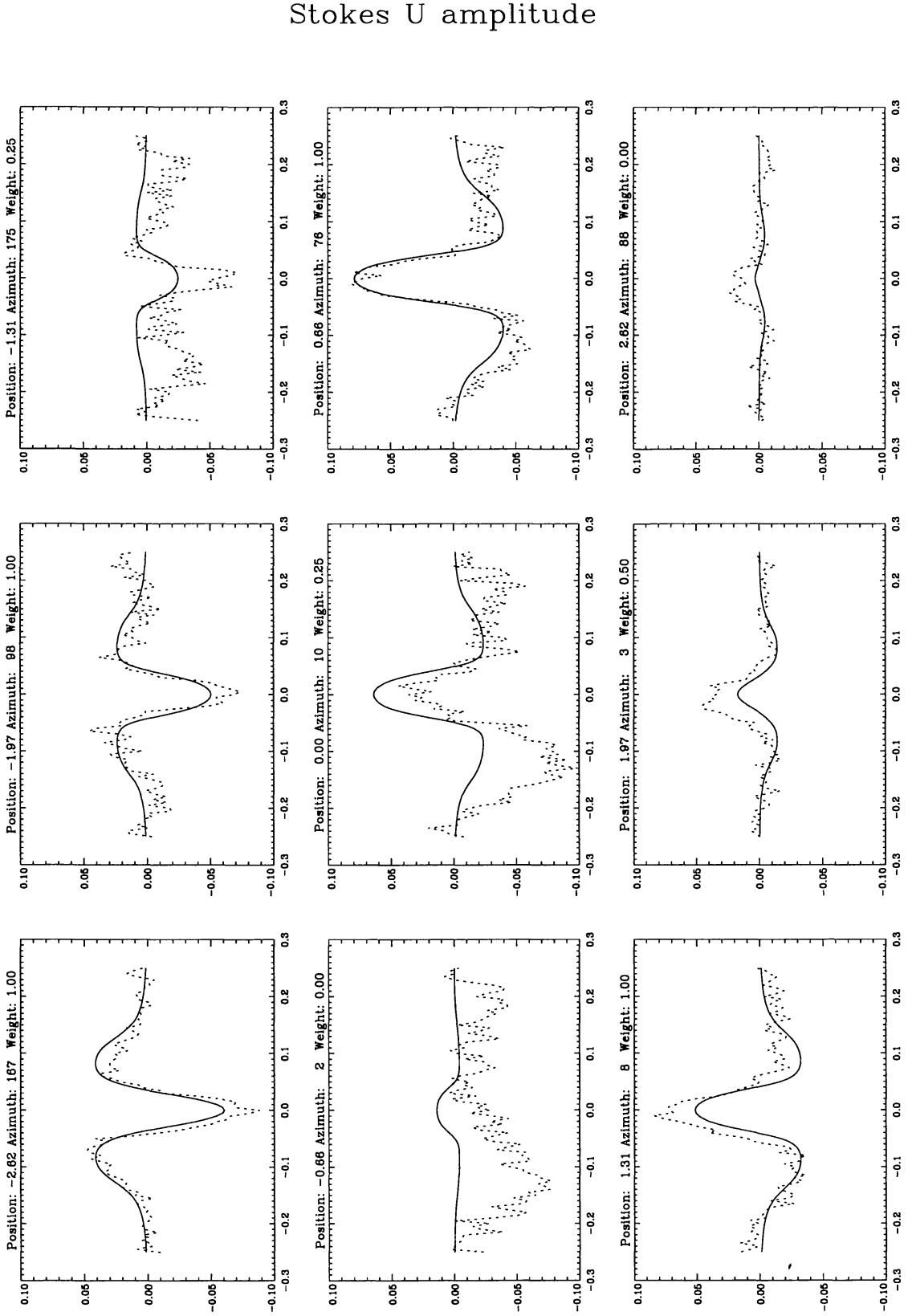

Fig. 8. The complete set of Stokes U profiles of the pore. The dotted lines are the measured spectra, the solid ones are calculated. The weight we used for the regression in Figure 7 is indicated on each plot.

for providing his inversion code which inspired us with certain improvements on our code. And finally, cordial thanks go to the organizers of the St. Petersburg workshop for their help and support.

References

Beckers, J.M., Schröter, E.H.: 1968, *Sol. Phys.* **4**, 142
Bonet, J.A., Sobotka, M., Vásquez, M.: 1994, *Astron. Astrophys.* **296**, 241
Brants, J.J., Steenbeck, J.C.M.: 1985, *Sol. Phys.* **96**, 229
Brants, J.J., Zwaan, C.: 1982, *Sol. Phys.***80**, 251
Bumba, V.: 1967, *Sol. Phys.* **1**, 371
Keller, C.U.: 1995, *Nature* **359** 307
Keller, C.U., Johannesson, A.: 1995, *Astron. Astrophys. Suppl.* **110**, 565
Muller, R.: 1992, in J.H.Thomas, N.O.Weiss (eds), *Sunspots: Theory and Observations*, Kluwer, p. 175
Muglach, K., Solanki, S.K., Livingston, W.C.: 1994, in R.J.Rutten, C.J.Schrijver (eds), *Solar Surface Magnetism*, Kluwer, p. 127
Rossbach, M, Schröter, E.H.: 1970, *Sol. Phys.* **12**, 95
Soltau, D.: 1993, Dissertation Universität Freiburg
Sütterlin, P.: 1991, Diplomarbeit Universität Freiburg
Sütterlin, P., Thim, F., Schröter, E.H.: 1994, in M.Schüssler, W.Schmidt (eds), *Solar Magnetic Fields*, Cambridge university Press, p. 213
Thim, F.: 1993, Diplomarbeit Universität Freiburg
Vernazza, J.E., Avrett, E.H., Loeser, R.: 1976, *Astrophys. J. Suppl.* **30**, 1